

Printing soft matter in three dimensions

Ryan L. Truby^{1,2} & Jennifer A. Lewis^{1,2}

Light- and ink-based three-dimensional (3D) printing methods allow the rapid design and fabrication of materials without the need for expensive tooling, dies or lithographic masks. They have led to an era of manufacturing in which computers can control the fabrication of soft matter that has tunable mechanical, electrical and other functional properties. The expanding range of printable materials, coupled with the ability to programmably control their composition and architecture across various length scales, is driving innovation in myriad applications. This is illustrated by examples of biologically inspired composites, shape-morphing systems, soft sensors and robotics that only additive manufacturing can produce.

Additive manufacturing, which encompasses a broad range of light- and ink-based printing techniques that allow the digital design and fabrication of three-dimensional (3D) objects, is transforming the science and engineering of advanced materials. Unlike conventional manufacturing methods that require moulds, dies or lithographic masks, digital assembly makes it possible to rapidly turn computer-aided designs into complex 3D objects on demand. Several techniques have been introduced over the past four decades^{1–7} that use industrial and desktop 3D printers to pattern soft materials. So far, commercial 3D printers have focused mostly on rapid prototyping of 3D objects. Most printing platforms use soft materials in one of three forms: photocurable resins^{2,3}, polymer powders^{4,5} or thermoplastic monofilaments⁶.

To unleash the vast potential of additive manufacturing, new materials and printing methods are needed that enable fabrication involving different materials at high speeds and with high precision over large build volumes. The scientific impetus for this technology is the drive to create architected matter that has qualitatively new properties, but this requires unprecedented control over the material's composition, structure, function and dynamics. By providing the ability to make products on demand in both low production runs and with customized form factors (such as size and shape), additive manufacturing provides a strong economic driver for adoption across a range of industrial sectors, such as aerospace, automotive, biomedical, robotics, and much more. From the manufacturing of plastic air ducts in aircraft to customized orthodontics, orthotics and hearing-aid shells, 3D printing is beginning to disrupt conventional manufacturing and supply chains across the world⁸.

In this Review we describe soft matter and introduce the light- and ink-based 3D printing techniques that are used to pattern such materials, with an emphasis on enhancing feature resolution, printing speed and the integration of different materials. We then highlight several emerging applications, including biologically inspired architectures for structural applications, shape-morphing structures, soft sensors and robots. Discussion of the many advances in 3D-printed biomedical devices^{9,10}, human tissues^{11,12–17}, and optical¹⁸ and electronic devices^{19–22} are beyond the scope of this Review, but there are already several excellent reviews that cover these areas. Finally, we share our perspective on the future directions with the potential for greatest societal impact.

Defining soft matter

Soft matter encompasses a broad range of synthetic and biological materials, including thermoplastic, thermosetting and elastomeric

polymers, hydrogels, liquid crystals and granular media²³. These materials are composed of basic building blocks — polymer chains, molecules or particles — that can be easily moved and so allow deformation under shear or other external forces. During 3D printing, the constituents are solidified into 3D architectures with elastic moduli that span orders of magnitude, from squishy hydrogels (10–100 kPa)¹¹ to rigid epoxy composites (>10 GPa)²⁴. The viscoelasticity, compliance (ease of deformation) and toughness of the printed materials may also be tailored to enable them to readily undergo (and even recover from) large deformations.

Overview of 3D printing

In 3D printing, a computer-controlled translation stage typically moves a pattern-generating device, either in the form of laser optics or an ink-based printhead, to fabricate objects a layer at a time. During the printing process, patterned regions composed of resins, powders or inks are solidified to yield the desired 3D form. Simply put, these printed objects are tangible representations of the digital designs that guide the printing process. Since the inception of 3D printing, several basic printing techniques have been introduced (Fig. 1), enabling technological advances that range from rapid prototyping to the additive manufacturing of finished parts^{2–6}. The specific patterning and solidification process used by a given 3D printing method define the minimum feature size it can create (Fig. 2a) and the type of printable soft materials it can use (Fig. 2b–g). Variations on these basic methods have largely focused on improving printing resolution²⁵ and speed^{26–28}, and on integrating multiple materials in a given printed part^{15,29–35}.

Light-based 3D printing

The first 3D printing methods to emerge used light to sculpt objects through either the stereolithography (SLA) of photocurable resins^{2,3}, or the selective laser sintering (SLS) of polymeric powders⁵ (Fig. 1a,b). In SLA, a liquid resin is selectively photopolymerized by a rastering laser. Once a layer has been printed, a new layer of liquid resin is introduced and subsequently crosslinked in locally illuminated regions. This process is repeated, layer by layer, until the desired 3D object is complete. Newer methods, including digital projection lithography (DLP)^{26,36}, continuous liquid interface production (CLIP)²⁷ and two-photon polymerization (2PP)²⁵, are all based on this basic concept. However, unlike SLA, which relies on point-source illumination to pattern one volume element (a 'voxel') at a time, DLP and CLIP enable an entire

¹John A. Paulson School of Engineering and Applied Sciences, and ²Wyss Institute for Biologically Inspired Engineering, Harvard University, Cambridge, Massachusetts 02138, USA.

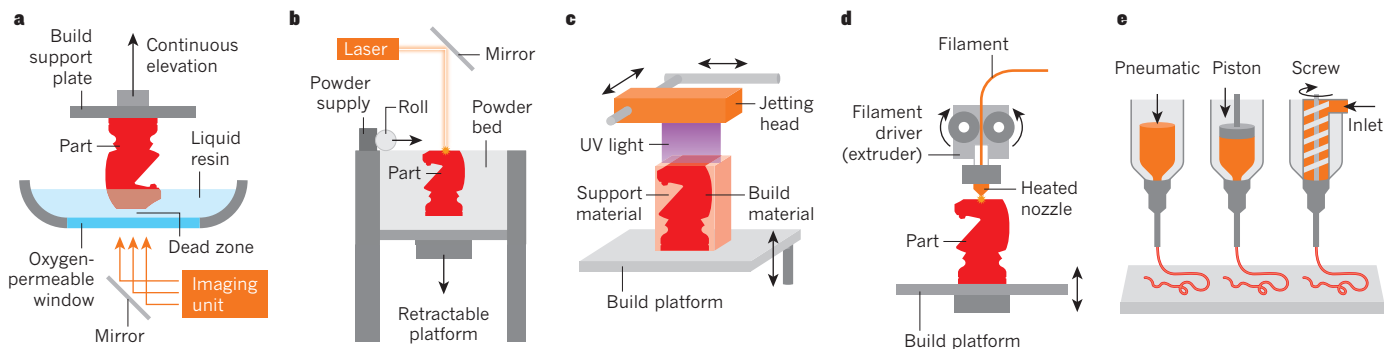


Figure 1 | Common light- and ink-based 3D printing methods. **a**, The light-based 3D printing method known as continuous liquid interface production. (Diagram adapted from ref. 27.) **b**, Light-based selective laser

sintering of powders. **c**, Light- and ink-based photocurable inkjet printing of photopolymerizable resins. **d**, Ink-based fused deposition modelling of thermoplastic filaments. **e**, Direct ink writing using viscoelastic inks.

layer to be solidified by using micro-mirror array devices²⁶ or dynamic liquid-crystal masks³⁶ to project a mask pattern onto the liquid-resin reservoir. As such, both DLP and CLIP are much faster than SLA. By contrast, 2PP provides the highest lateral resolution (around 100 nm) in 3D printed parts by taking advantage of the squared point-spread function associated with the two-photon absorption of light of wavelength λ , which is confined to a tightly focused voxel with dimensions on the order of λ^3 (ref. 25). But as with all 3D printing methods, there is an inherent trade-off between printer resolution (Fig. 2a), build volume and speed. This means that 2PP can be used to fabricate highly complex microarchitectures, but the overall dimensions are typically limited to 1 cm³ (Fig. 2b)^{25,37–39}, whereas CLIP can readily produce complex parts with overall dimensions exceeding 100 cm³ (Fig. 2c) with minimal surface roughness, but with lower lateral resolution²⁷. However, none of these methods currently allows multiple materials to be patterned in a single build sequence.

In SLS, polymer particles in a powder bed are locally heated and fused together by a rastering laser^{5,40}. After a layer has been printed, a new layer of powder is spread across the bed and locally sintered. To facilitate spreading, granulated powders are used that typically have diameters between 10 μm and 100 μm . The non-fused regions in the powder bed serve as a support material during the building process. After the 3D object has been completed and removed from the powder bed, the loose powder is removed and recycled⁵. A representative part produced by the SLS of nylon powder is shown in Fig. 2d. The minimum feature size achieved by this printing method is around 100 μm , which is a few times larger than the typical particle size in the powder bed.

Ink-based 3D printing

Although light-based printing methods provide the highest feature resolution, they are limited to patterning with either photopolymerizable resins, which yield only rigid thermoset polymers, or thermoplastic polymer powders. Ink-based 3D printing methods, in contrast, can pattern myriad soft materials in the form of printable inks that are formulated from a wide range of molecular, polymeric or particulate species. These can be chosen to achieve the desired flow behaviour — characterized by the ink's viscosity, surface tension, shear yield stress, and shear elastic and loss moduli — required for either droplet- or filament-based printing.

In droplet-based printing methods, soft materials are deposited by printheads similar to those used in the printing of 2D documents. Several 3D printing methods use this approach, including direct inkjet printing⁴¹, hot-melt printing¹⁹ and inkjet printing on a powder bed⁴. Inks for these approaches are composed of low-viscosity fluids. For example, in hot-melt printing, wax-based inks are heated during droplet formation and then solidify on impact. Other inkjet printers combine ink- and light-based printing in one platform: photocurable resins, for example, are polymerized when they are printed by illumination with an ultraviolet light source (Figs 1c and 2e). In an alternative to depositing the component material itself, binder solutions can be jetted onto powder beds to locally fuse particles in a method akin to SLS printing^{4,19}. In all these ink-based printing approaches, drop formation depends on both the properties of the ink material and the printing parameters, including the ink's density (ρ), viscosity (μ), surface tension (γ) and characteristic droplet length (L , which in most cases is the drop diameter), as well as

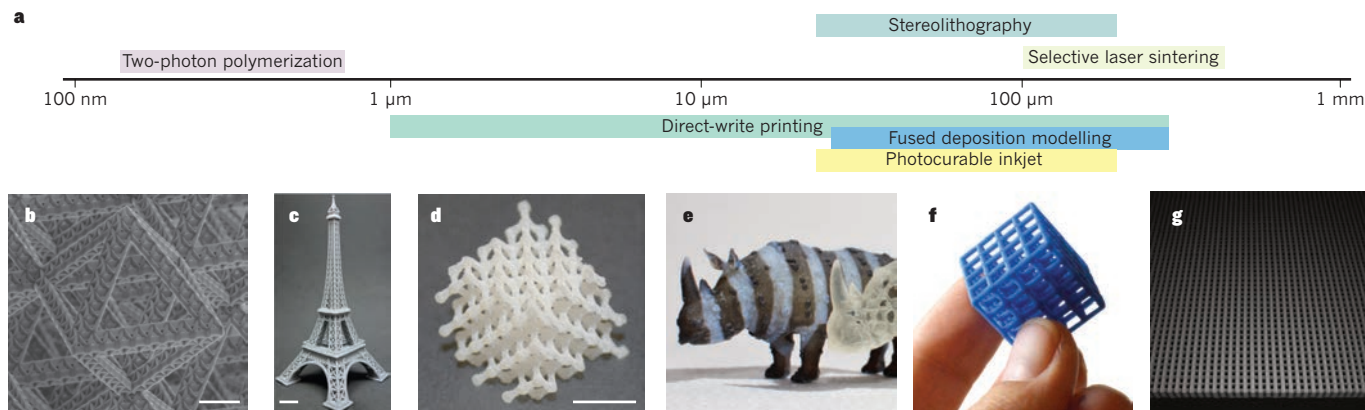


Figure 2 | Sizes and shapes of typical 3D-printed objects. **a**, Coloured bars show the minimum size ranges of patterned features produced by several light- and ink-based printing methods. **b–g**, Examples of polymer constructs printed by: **b**, two-photon polymerization (hierarchical octet truss; scale bar, 25 μm ; photo courtesy of J. Greer); **c**, continuous liquid interface production (Eiffel Tower; scale bar, 10 mm; adapted from ref. 27);

d, selective laser sintering (hierarchical lattice; scale bar, 10 mm; adapted from ref. 40); **e**, inkjet printing of photopolymerizable resins (multimaterial rhinoceros; adapted from ref. 54); **f**, fused deposition modelling (3D lattice; photo courtesy of S. Bernier, Zortrax); **g**, direct ink writing (3D epoxy lattice with 250- μm features; photo courtesy of B. Compton and J. Lewis).

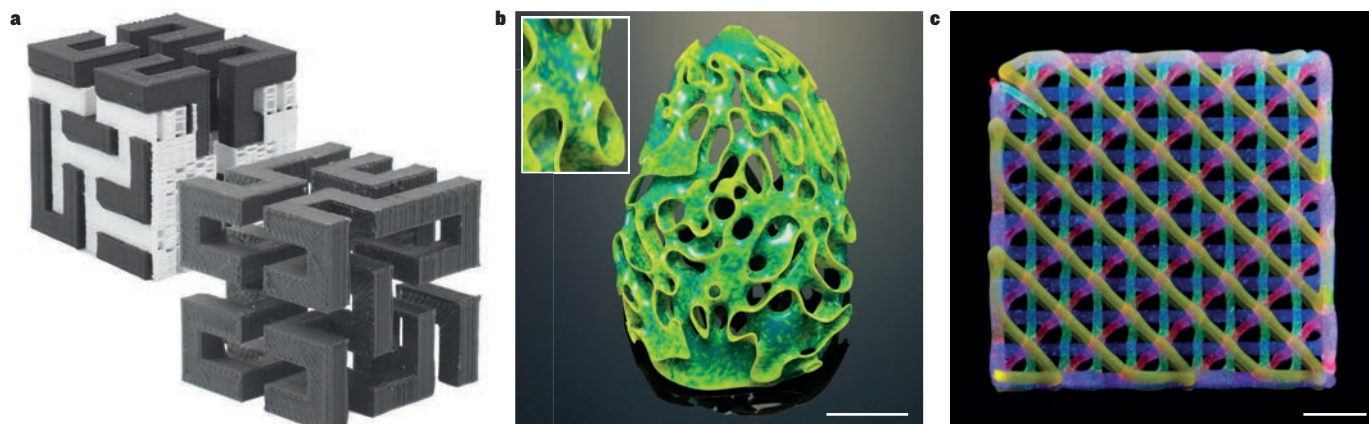


Figure 3 | Techniques for the fabrication of complex structures. **a**, The white sacrificial support material in an FDM-printed part (back) is removed to reveal a Hilbert cube with numerous overhangs (front). (Photo courtesy of Polymaker.) **b**, A conceptual artwork by N. Oxman produced by multimaterial inkjet printing (scale bar, 10 cm). The inset shows the complex distribution

of materials in the structure. (Photo courtesy of N. Oxman.) **c**, Multimaterial elastomeric lattice produced by direct ink writing. The 3D microlattice (1 cm × 1 cm × 1 mm) is produced by sequential printing layers composed of silicone-based inks dyed with blue, red, green and yellow fluorophores, each deposited by a separate nozzle (scale bar, 2 mm; adapted from ref. 15).

the velocity of the ejected droplet (v) and the nozzle diameter (d). These parameters must all be tightly controlled to achieve the right balance between viscosity, surface tension and inertial forces. This is usually captured by the dimensionless Z parameter, given as the inverse of the Ohnesorge number (Oh), that relates inertial and surface-tension forces to viscous forces as follows:

$$Z = 1/Oh = Re/\sqrt{We} = [\sqrt{(\rho\gamma L)}]/\mu \quad (1)$$

where Re and We are the Reynolds and Weber numbers, respectively^{41,42}. If viscous forces dominate (low Z), the ink droplets will not form during printing. If inertial or surface-tension forces dominate (high Z), ejected droplets will be prone to splashing or breaking up into multiple satellite droplets during printing, so print fidelity will diminish. Generally, ideal droplet formation occurs when Z is between 1 and 10, and the droplet velocity is at least equal to $\sqrt{(4\gamma/\rho d)}$. The fluid dynamics involved in drop formation, wetting and spreading play an important, yet limiting, role in defining the surface roughness and minimum feature size (~ 10 – 100 μm) of the printed objects. Typical values for μ , L and v are 2–20 mPa s, 10–30 μm and 1–10 m s^{-1} , respectively. All this means that it is difficult to jet (without clogging) complex fluids, such as concentrated polymer solutions, or solutions that contain filler particles that exceed 100 nm in diameter, or at concentrations above a few per cent. Nevertheless, these difficulties are in many cases outweighed by the huge advantages of inkjet-based methods arising from their highly sophisticated printhead designs — state-of-the-art multinozzle arrays may have thousands of nozzles that can deliver more than 100 million drops per second with picolitre volumes — and their ability to print using different materials⁴¹.

Compared with droplet-based methods, 3D filament printing allows a broader range of ink designs, feature sizes and geometries^{6,43}. In this approach, soft materials are deposited as a continuous filament but still a layer at a time. In the earliest form, known as fused deposition modelling (FDM), thermoplastic filaments are fed through a hot extrusion head during printing and then solidify as they cool below their glass transition temperature^{6,44} (Fig. 1d). Several types of thermoplastic polymer can be patterned by this approach, including the widely used acrylonitrile butadiene styrene (ABS), polylactic acid (PLA) and polycarbonate (Fig. 2f). The polymer filaments can also be filled with particles, such as carbon black, to enhance the functionality of the printed parts⁴⁵. Given their ease of use and compatibility with common materials, desktop FDM printers have helped to drive the ‘maker revolution’ in the past decade.

One important alternative to FDM printing is the direct ink writing (DIW) of viscoelastic materials under ambient conditions⁴³ (Fig. 1e).

Crucial to its success has been the development of concentrated polymer^{46–49}, fugitive organic (used as sacrificial materials)^{50,51}, and filled epoxy²⁴ inks, which have fluid properties that enable the printing of complex 3D architectures (Fig. 2g). These yield-stress fluids are well described by the Herschel–Bulkley model⁵²:

$$\tau = \tau_y + K\dot{\gamma}^n \quad (2)$$

where τ is the shear stress, K is the consistency $\dot{\gamma}$ is the shear rate, and n is the flow index ($n < 1$ for shear-thinning fluids). Typical values for the apparent ink viscosity, minimum filament diameter and printing speed are 10^2 – 10^6 mPa s (depending on the shear rate), 1–250 μm (~ 10 – 100 times higher than the characteristic size of the building blocks for a given ink), and 1 mm s^{-1} to 10 cm s^{-1} , respectively. To induce flow through the nozzle, the applied stress in the printhead must exceed the yield stress, τ_y , of these inks so that they fluidize and then, when they exit the nozzle, rapidly recover their original values of τ_y and the shear elastic modulus, G' (ref. 43).

In some cases, additional processing steps (such as photopolymerization or thermal curing) may be required to fully solidify the printed parts. When these steps are decoupled from the printing process, it can be difficult to build truly 3D objects, as the underlying printed layers may not fully support the subsequent layers. However, these problems can be overcome by using printheads coupled with ultraviolet LEDs⁵³ or heated build chambers.

Multimaterial 3D printing

The complexity and functional performance of 3D printed objects can be enhanced by printing different materials together, but this requires a high degree of spatial and compositional precision. Light-based methods are currently not well suited to such multimaterial fabrication, because it is difficult to dynamically alter the composition of a liquid photopolymer reservoir or powder bed during printing^{29,30}. By contrast, ink-based printing methods such as FDM, inkjet printing and DIW can easily be used for multimaterial 3D printing.

Both FDM and inkjet printers are capable of printing primary building materials alongside sacrificial materials that support overhanging or spanning features. An exemplary Hilbert cube produced by FDM is shown in Fig. 3a before and after the removal of the white support material. Inkjet printing enables voxel-by-voxel patterning of multiple materials, using a full-colour palette and photopolymer resins whose backbone composition, side-group chemistry and crosslink density can be systematically varied to produce regions with different mechanical properties (Fig. 3b), at a higher resolution than FDM printing can achieve^{35,54}.

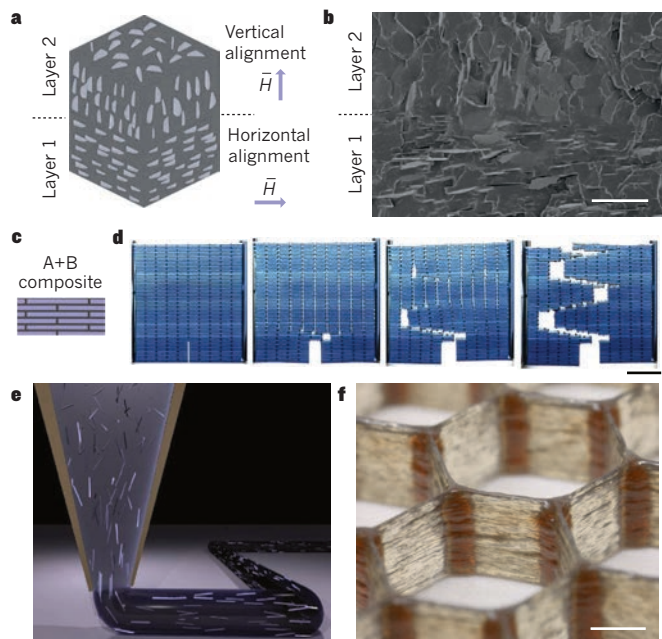


Figure 4 | Bio-inspired composites. **a, b**, 3D magnetic printing of platelet-reinforced composites, in which a magnetic field is used to induce the desired platelet orientation, and digital light projection (DLP) is used to locally photopolymerize oriented voxels (**a**). This motif mimics the layered architecture of abalone shells (**b**; scale bar, 25 μm ; both **a** and **b** are adapted from ref. 63). **c, d**, Inkjet printing of rigid (A) and compliant (B) material in a ‘bricks and mortar’ structure that resembles nacre or bone (**c**). Toughening occurs owing to delocalized load transfer away from the crack tip and crack deflection (**d**; scale bar, 20 mm; adapted from ref. 64). **e, f**, Direct ink writing of fibre-filled epoxy composites in a cellular motif inspired by balsa wood. The anisotropic fibre filler aligns in the shear and extensional flow field in the tapered nozzle during printing (**e**). An epoxy-based composite with hexagonal cells, in which carbon fibres align along the printing direction, that is, horizontally in the cell walls (**f**; scale bar, 2 mm; adapted from ref. 24).

At present, DIW⁴³ offers the broadest spectrum of printable materials, including structural^{11,47,48}, electrical^{33,55} and biological¹⁵ materials. Multimaterial DIW can be achieved either by using multiple (single-nozzle) printheads (Fig. 3c), each of which houses a different ink composition¹⁵, or by using microfluidic printheads that allow for switching³¹, mixing³², core-shell printing³³, or printing multiple filament arrays in a single pass²⁸. Microfluidic switching nozzles can swap between two different inks when required³¹, whereas mixing nozzles can be used to print materials with tunable gradients of mechanical, conductive or other material properties³². Core-shell printheads yield filaments that contain concentric layered materials³³. Finally, multinozzle printheads separate a single ink stream into 2^n streams, where n is the number of bifurcating generations in the printhead, allowing a dramatic reduction in build time (for example, a part requiring 24 h to build using a single nozzle can be printed in 22 min using a 64-nozzle array)²⁸. By using dual multinozzle arrays, two disparate inks can be patterned simultaneously. However, these multinozzle arrays consist of nozzles that are relatively large (100–200 μm in diameter), and they are not individually addressable like those used in inkjet printing. Finally, there is growing interest in directly writing inks into matrix materials by a process known as embedded 3D printing, which enables truly free-form fabrication of soft materials^{51,55,56}. These variants of DIW offer considerable flexibility in the types and motifs of shapes that can be printed.

Architected soft matter

The term ‘architecture’, which normally refers to the design and construction of buildings, is increasingly being used to describe materials that have optimized composition and topology. With 3D printing, it has become possible to fabricate architected matter from

an ever-broadening palette of soft materials in a programmable way, opening up a new design space for scientists and engineers^{8,16,19,21,57–59}. There are many noteworthy examples, but here we are focusing on advances in printing biologically inspired composites, shape-morphing systems, soft sensors and robotics.

Bio-inspired composites

Natural composite materials, such as nacre⁶⁰, bone⁶¹ and wood⁶², are typically held together by the organization of platelet or fibre reinforcement in complex architectures. These features help them achieve remarkable properties that exceed the sum of their parts, often combining stiffness, low density and high specific strength. They may also have energy-dissipation capabilities that lead to graceful failure, so they remain functional even when they start to fail. Inspired by these natural examples, researchers have focused on printing synthetic analogues in which the spatial organization and alignment of reinforcing fillers or printed features within polymer matrices are well controlled.

In one promising approach, external magnetic fields are used to control platelet orientation^{34,63} in photopolymerizable liquid resins, which are patterned layer-by-layer using DLP (Fig. 4a,b). The printer is modified by placing three electromagnetic solenoids around its periphery, which generate a magnetic field that aligns iron oxide-coated platelets (about 10 μm in length) suspended in the liquid photopolymer resin, along a prescribed vector in 3D space. The oriented voxels, whose minimum lateral dimension is about 100 μm , are photopolymerized to lock in the desired platelet orientation by crosslinking the surrounding matrix. Tensile testing reveals that printed objects with oxide platelets aligned parallel to the applied load exhibit higher stiffness (+29%), hardness (+23%) and strain at rupture (+100%) than those with orthogonally aligned platelets, and are twice as stiff as printed polymer matrices devoid of platelets. By coupling dynamic masking with magnetic alignment, filler particles can adopt different orientations within or between each layer (Fig. 4a). One architecture mimics the calcite prismatic and aragonite ‘bricks and mortar’ layers found in abalone shells⁶³ (Fig. 4b). There are limitations, however, owing to the sedimentation of dense fillers in the liquid resin during printing, which can lead to unintended compositional gradients, and excluded volume effects may hinder the orientation of filler in more concentrated systems.

Another approach to creating bricks-and-mortar architectures relies on multimaterial inkjet printing of rigid and compliant photocurable resins⁶⁴ (Fig. 4c). Samples composed entirely of either rigid (material A) or compliant (material B) material — the ‘bricks’ and ‘mortar’, respectively, in Fig. 4c — were printed, cured and characterized. Their respective yield strengths were 0.5 and 15 MPa, with a stiffness ratio, E_A/E_B , of about 1,500. In both cases, cracks initiate in the notched regions and propagate smoothly through the pure samples. Bio-inspired composites were also fabricated by printing rigid bricks coated with a thin compliant layer (about 250 μm thick). These architectures emulate the fracture-propagating, high-toughness properties of nacre and bone (Fig. 4d). Both delocalized load transfer away from the crack tip and crack deflection through the compliant coating enhance the fracture toughness of these printed composites. However, a little mixing (3–4%) occurs between layers during the printing process, reducing the effective stiffness ratio by nearly two orders of magnitude⁶⁴. To improve performance further, resin chemistries with more disparate baseline properties are needed to retain good interlayer adhesion during printing.

Some structural applications use fibre-filled epoxy composites in which the reinforcing fillers are in either discrete or continuous form. Inspired by balsa wood — which rivals the best engineering materials in terms of specific bending stiffness and strength — synthetic cellular architectures have been created by DIW using an epoxy resin-based ink filled with short carbon fibres. During the printing process, these anisotropic fillers align under the shear and extensional flow field that develops in the nozzle (Fig. 4e), resulting in enhanced

stiffness in the thermally cured composite along the printing direction (Fig. 4f). Printed tensile bars containing fibres aligned parallel to the applied load exhibited stiffness values nearly equivalent to those of wood cell walls, and 10–20 times higher than most commercial 3D-printed polymers²⁴. One shortcoming of DIW is its inability to fabricate continuous fibre-reinforced composites, but this is possible using a variant of FDM in which continuous fibres are embedded in thermoplastic matrices⁶⁵.

The patterned features and complexity of 3D-printed architectures do not yet match those found in nature. But there is scope to extend these boundaries and create materials with properties that meet or even exceed those of biological materials. If new materials and printing methods were capable of encoding a richer range of compositional and structural hierarchy across length scales, especially around 100 nm, this would accelerate innovation.

Shape-morphing systems

There is a growing emphasis on designing soft matter that has intrinsically programmed responsiveness, adaptability and other functionality. Materials of this sort include structural metamaterials, such as lightweight, ultrastiff cellular trusses^{37,66}, topology-optimized auxetic⁴⁷ and negative-stiffness lattices⁶⁷, and bistable structures that store energy through mechanical deformation⁴⁸. A related and currently active research direction focuses on materials that autonomously change their shape. The term ‘4D printing’ is often used to describe the fabrication of 3D objects that can then change their shape over time in response to an environmental stimulus. Such shape-morphing systems often respond autonomously to light, heat or moisture, and are sometimes used in smart textiles⁶⁸, robotic systems⁶⁹ and biomedical devices⁷⁰.

In one approach, inkjet printing was used to create shape-changing architectures by patterning a light-absorbing ink onto a prestrained polystyrene substrate. Under infrared illumination, the underlying substrate was locally heated in the patterned regions, which acted like hinges to induce an autonomous, origami-like shape change⁷¹ (Fig. 5a,b). Building on this concept, linear structures with hinges that can swell have been created by multimaterial printing. These can self-assemble into various predetermined 3D shapes when immersed in water^{72,73} (Fig. 5c). In another approach, shape-memory polymers have been printed to create stimuli-responsive architectures^{74–77}. These constructs are fabricated in their intended (final) form before being warmed to a temperature above the glass transition temperature (T_g) of the hinges. They are then mechanically deformed to a prefolded or other initial shape, and cooled below T_g to lock the hinges in place. Upon reheating the printed object above T_g , its shape transforms back to the originally printed form^{74–77} (Fig. 5d). So far, only simple shape changes have been demonstrated.

Biomimetic 4D printing offers an easy route to encoding complex shape changes in hydrogel-based composites⁴⁹. Inspired by the nastic movements of plants^{78,79}, in which plants respond non-directionally to changes in stimuli such as heat or humidity, hydrogel inks containing stiff cellulose fibrils were designed to mimic the composition of plant cell walls. These anisotropic fibrils align along the printing direction, so it is possible to define the swelling and elastic anisotropies required to induce the desired shape change upon immersion in water by controlling the print path. Printing bilayer patterns in floral forms composed of five petals in either a 90°/0° or –45°/45° configuration can induce simple changes in curvature, such as bending and twisting, respectively, when the initially flat forms swell in water (Fig. 5e,f). A theoretical framework developed to solve the inverse problem (in which one wants to design a final form but the required print path is unknown) makes it possible to move beyond these simple structures to print much more complex shape-morphing architectures, including some that mimic orchids and calla lilies⁴⁹. The modularity of the composite inks used to fabricate these structures should make it possible to incorporate other hydrogel matrix and anisotropic filler chemistries to encode

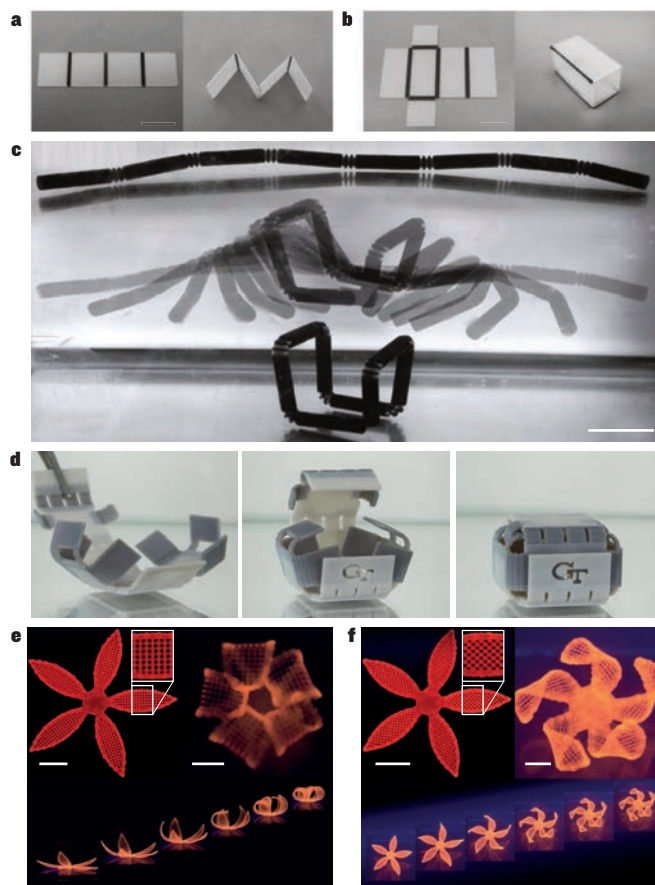


Figure 5 | Stimuli-responsive, morphing architectures. **a, b**, Prestrained polystyrene substrate with inkjet-printed hinges made of carbon black ink (**a**), which autonomously folds into a 3D shape (**b**) when illuminated with infrared light (scale bars, 10 mm; adapted from ref. 71). **c**, 4D-printed composite with swellable hinges (top) that self-assembles from a linear into a box-like structure (bottom) when immersed in water (scale bar, 5 cm; adapted from ref. 72). **d**, A 4D-printed unfolded box composed of shape-memory polymers that folds back into its original conformation when immersed in warm water (adapted from ref. 76). **e, f**, Biomimetic 4D printing of hydrogel composites containing anisotropic cellulose fibrils that orient along the printing direction. They undergo anisotropic swelling to programmably change shape when immersed in water. The printed bilayer lattices transform into flowers, whose petals either bend or twist when the bilayer orientations are 90°/0° (**e**) or –45°/45° (**f**) (scale bars, 5 mm; insets, 2.5 mm; adapted from ref. 49).

responses to other stimuli, such as light, heat and pH.

The focus is now turning to strategies for creating shape-morphing architectures that transform rapidly and provide significant actuation forces. However, the response times of shape-morphing structures are usually slow, and the structures tend to be mechanically weak — limitations that will need to be overcome if practical applications are to be developed.

Soft sensors and robots

Soft sensors, actuators and robots are improving human–machine interactions across a broad spectrum of applications. A central requirement for this is the ability to integrate soft materials with disparate mechanical and electrical properties in customized form factors^{80–82}; 3D printing is particularly well suited to produce such soft devices and systems.

Consider, for example, soft strain sensors, which are typically composed of a deformable conducting material that is patterned onto, attached to or encapsulated within an insulating, conformable, stretchable soft matrix^{21,83–85}. Embedded 3D printing has recently been used to fabricate highly stretchable strain sensors composed of a conductive carbon ink patterned in an elastomeric matrix⁵⁵ (Fig. 6a).

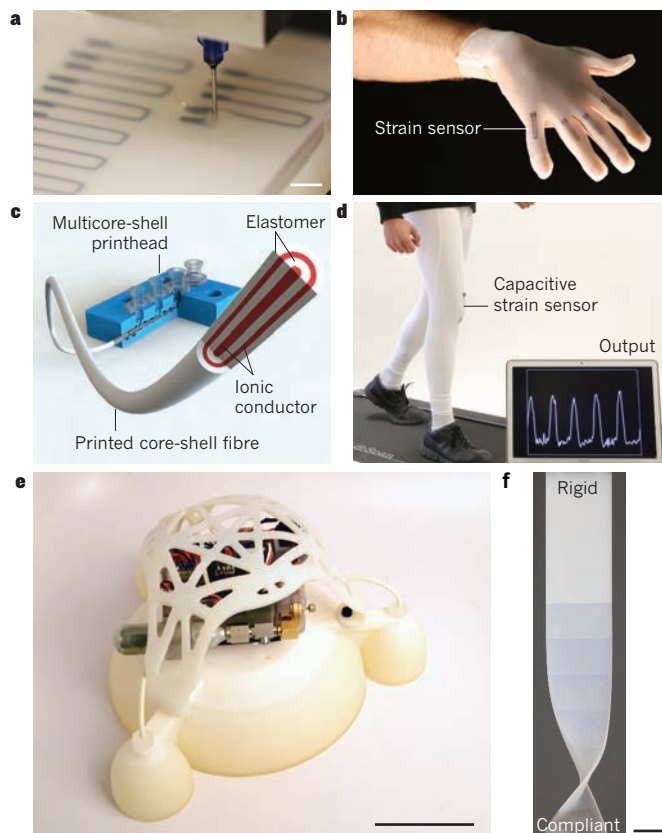


Figure 6 | Soft sensors, actuators and robots. **a, b**, Soft strain sensors are patterned directly in a free-form nature in an elastomeric matrix by ‘embedded 3D’ printing (**a**; scale bar, 5 mm). Strain sensors embedded into a glove-shaped, elastomeric matrix enable proprioceptive sensing of joint bending (**b**); (**a** and **b** adapted from ref. 55). **c, d**, Capacitive soft sensors based on ionically conductive inks are printed using a multicore-shell printhead, which produces a fibre sensor composed of concentric layered materials. Concentric shells of ionically conductive ink (red) are encapsulated by dielectric, elastomer layers (white) (**c**). Soft capacitive sensors printed with multicore-shell printheads can be integrated into textiles for wearable technologies (**d**); (**c** and **d** adapted from ref. 33). **e, f**, A soft-bodied robot powered by combustion can carry heavy hardware (**e**; scale bar, 10 cm). The printed body has a graded modulus, enabling the compliant materials needed for locomotion to interface seamlessly with the rigid materials of the auxiliary hardware (**f**; scale bar, 10 mm); (**e** and **f** adapted from ref. 35).

The resulting hairpin sensors exhibit increased electrical resistance when they are stretched. The approach was then used to fabricate a wearable glove containing embedded strain sensors (Fig. 6b), which provide resistive feedback when the fingers are bent, making them ideal for training and rehabilitation purposes. The free-form nature of the embedded 3D printing allows the rapid fabrication of highly complex soft sensors⁵⁵, and avoids the delamination issues that typically arise for soft sensors made by conventional moulding and lamination processes^{86–88}. Other approaches for printing soft sensors have relied on directly printing elastomers, such as fluorinated rubbers with conductive particle fillers^{89,90}. One drawback of these sensors, however, is that they exhibit hysteresis — there is a time lag between the break-up and the reformation of the conductive particle networks during a given strain cycle^{55,89}.

The limitations caused by hysteresis can be overcome by integrating liquid metal (such as eutectic gallium indium, eGaIn) into soft sensing architectures^{86–88}. However, the high surface tension of eGaIn and other liquid metals poses serious challenges for printing⁹¹, so ionically conductive inks are being explored. These have recently been successfully encapsulated in a highly extensible elastomeric matrix and used to produce textile-mounted, capacitive fibre sensors³³. This

required a specially designed multicore-shell printhead that was capable of printing filaments composed of concentric conductive features separated by highly stretchable elastomer shells (Fig. 6c). The capacitance, resistance and decay time of these capacitive fibre sensors were measured as a function of strain, as required for soft joint proprioceptive sensing³³ (Fig. 6d).

Soft actuators derived from swellable hydrogels^{92–94}, granular media⁹⁵ and electroactive polymers⁹⁶ have all been fabricated so far. Of these, the most widely used are fluidic elastomer actuators (FEAs), which consist of a network of open channels within elastomeric composites^{80,82,97}. These embedded pneumatic networks inflate when filled with a fluid, inducing the desired actuating motion. Although FEAs are typically fabricated by a multistep moulding process, SLA printing of silicone-based photo-crosslinkable resins has recently been demonstrated. Using this method, FEAs can be designed with arbitrarily complex fluidic chambers to drive multidirectional actuation when inflated⁹⁸. Methods based on DIW have produced elastomeric actuators that serve as simple haptic feedback devices⁹⁹, and more complex FEAs have been produced by multimaterial inkjet printing¹⁰⁰. These initial demonstrations reveal the power of digital design and manufacturing, but further research is required to develop compatible materials systems, printing methods and predictive models to optimize soft actuator mechanics.

A final point regarding the soft robotic systems developed so far is that most require tethers to ancillary hardware for control and power. The interfacing of bulky, rigid hardware components with robots constructed from soft materials is not straightforward, however. Here, 3D printing can come into its own, as illustrated by the recent example of a soft robot that can jump being powered by combustion (Fig. 6e). The body of the robot was created using multimaterial inkjet printing to pattern multiple photopolymer layers of varying compliance. The resulting graded elastic modulus (Fig. 6f) meant that the robot body smoothly transitioned from a rigid core to a soft exterior, improving the interface between the robot’s body and the on-board power and control hardware needed for propulsion³⁵. Coupling 3D printing to appropriate design in this way offers tremendous opportunities for integrating soft control, power and sensing elements to create fully autonomous soft robots and machines¹⁰¹.

Future directions

Together, digital design and additive manufacturing have huge potential. The pace of discovery and innovation is rapidly accelerating as 3D, and now 4D, printing methods are increasingly embraced by the research community, as well as by industrial designers and engineers around the world.

From a scientific viewpoint, the ability to heterogeneously integrate soft materials with disparate mechanical, electrical and optical properties in topology-optimized architectures will lead to as-yet-unimagined performance. The examples highlighted above underscore the power of digital fabrication, but they should be viewed merely as a starting point. The current level of integration and sophistication in 3D-printed soft architectures is relatively simplistic; far more can be achieved by augmenting computer-aided design software with more informed inputs, perhaps based on materials genomics, multiscale modelling and topology optimization. But to fully take advantage of advanced generative designs, new 3D-printing platforms are also needed, so material composition and function can be controlled and designs integrated from the nanoscale to the macroscale. Closed-loop feedback control, coupled with machine vision and learning, would allow real-time error correction to ensure that 3D-printed objects conform to the target designs in a reproducible manner.

From a technological viewpoint, the adoption of 3D printing is being driven by applications that benefit from customization and have small production runs. Yet all the initial applications, such as patient-specific orthodontics, rely solely on the ability to create complex 3D shapes, often from a single material. The true power of

digital manufacturing will be realized only when form and function are fully integrated. If ‘complexity’ is inherently free in 3D-printed objects — that is, if it is as simple to print a cube as it is to print an architected form such as a miniature Eiffel Tower — then the ability to embed function is also necessarily free. It merely requires the integration of different materials across multiple length scales that give rise to unprecedented properties.

The rapidly changing digital landscape already pervades our lives and affects the way we communicate, connect and share information. But when will digital manufacturing cross the divide from niche applications to widespread adoption? This transition is already under way, as can be seen in the rapid growth in the use of desktop 3D printers by educators, makers and entrepreneurs, and the growing installation of more-sophisticated 3D printers for industrial manufacturing. Yet digital fabrication is hindered by several factors, including long build times, high cost and poor scalability. Moreover, most 3D printers have been developed for rapid prototyping, not manufacturing. For 3D printing to transform high-throughput manufacturing, either large numbers of low-cost desktop printers need to be deployed whose capabilities will improve over time, or new 3D printers must be developed that enable the continuous production of parts at high speeds. Either way, the convergence of advanced materials, hardware and software is inevitable, and these must be mastered in the twenty-first century. ■

Received 30 May; accepted 15 August 2016.

- Swainson, W. K. Method, medium and apparatus for producing three-dimensional figure product. US patent 4,041,476 (1977).
- Kodama, H. Automatic method for fabricating a three-dimensional plastic model with photo-hardening polymer. *Rev. Sci. Instrum.* **52**, 1770–1773 (1981).
- Hull, C. W. Apparatus for production of three-dimensional objects by stereolithography. US patent 4,575,330 (1986).
- Sachs, E. M., Haggerty, J. S., Cima, M. J. & Williams, P. A. Three-dimensional printing techniques. US patent 5,205,055 (1993).
- Beaman, J. J. & Deckard, C. R. Selective laser sintering with assisted powder handling. US patent 4,938,816 (1990).
- Crump, S. S. Apparatus and method for creating three-dimensional objects. US patent 5,121,329 (1992).
- Bradshaw, S., Bowyer, A. & Haufe, P. The intellectual property implications of low-cost 3D printing. *ScriptEd* **7**, 5–31 (2010).
- Lipson, H. & Kurman, M. *Fabricated: The New World of 3D Printing* (John Wiley, 2013).
- This book provides an overview of 3D printing and its impact on society.**
- Morrison, R. J. *et al.* Mitigation of tracheobronchomalacia with 3D-printed personalized medical devices in pediatric patients. *Sci. Transl. Med.* **7**, 285ra64 (2015).
- Gupta, M. K. *et al.* 3D printed programmable release capsules. *Nano Lett.* **15**, 5321–5329 (2015).
- Malda, J. *et al.* 25th anniversary article: Engineering hydrogels for biofabrication. *Adv. Mater.* **25**, 5011–5028 (2013).
- Derby, B. Printing and prototyping of tissues and scaffolds. *Science* **338**, 921–926 (2012).
- Villar, G., Graham, A. D. & Bayley, H. A Tissue-like printed material. *Science* **340**, 48–52 (2013).
- Mannoor, M. S. *et al.* 3D printed bionic ears. *Nano Lett.* **13**, 2634–2639 (2013).
- Kolesky, D. B. *et al.* 3D bioprinting of vascularized, heterogeneous cell-laden tissue constructs. *Adv. Mater.* **26**, 3124–3130 (2014).
- This paper demonstrates multimaterial 3D printing of soft materials with disparate chemical and mechanical properties.**
- Murphy, S. V. & Atala, A. 3D bioprinting of tissues and organs. *Nature Biotechnol.* **32**, 773–785 (2014).
- Ma, X. *et al.* Deterministically patterned biomimetic human iPSC-derived hepatic model via rapid 3D bioprinting. *Proc. Natl Acad. Sci. USA* **113**, 2206–2211 (2016).
- Gissibl, T., Thiele, S., Herkommer, A. & Giessen, H. Two-photon direct laser writing of ultracompact multi-lens objectives. *Nature Photonics* **10**, 554–560 (2016).
- de Gans, B.-J., Duineveld, P. C. & Schubert, U. S. Inkjet printing of polymers: state of the art and future developments. *Adv. Mater.* **16**, 203–213 (2004).
- Kong, Y. L. *et al.* 3D printed quantum dot light-emitting diodes. *Nano Lett.* **14**, 7017–7023 (2014).
- Rim, Y. S., Bae, S. H., Chen, H., De Marco, N. & Yang, Y. Recent progress in materials and devices toward printable and flexible sensors. *Adv. Mater.* **28**, 4415–4440 (2016).
- Kong, Y. L., Gupta, M. K., Johnson, B. N. & McAlpine, M. C. 3D printed bionic nanodevices. *Nano Today* **11**, 330–350 (2016).
- Jones, R. A. L. *Soft Condensed Matter* (Oxford Univ. Press, 2002).
- Compton, B. G. & Lewis, J. A. 3D-printing of lightweight cellular composites. *Adv. Mater.* **26**, 5930–5935 (2014).
- Cumpston, B. H. *et al.* Two-photon polymerization initiators for three-dimensional optical data storage and microfabrication. *Nature* **398**, 51–54 (1999).
- This paper lays the foundations for high-resolution 3D printing of soft materials.**
- Sun, C., Fang, N., Wu, D. M. & Zhang, X. Projection micro-stereolithography using digital micro-mirror dynamic mask. *Sensors Actuators A* **121**, 113–120 (2005).
- Tumbleston, J. R. *et al.* Continuous liquid interface production of 3D objects. *Science* **347**, 1349–1352 (2015).
- This paper details a method for 3D printing of photopolymerizable resins at high speed.**
- Hansen, C. J. *et al.* High-throughput printing via microvascular multinozzle arrays. *Adv. Mater.* **25**, 96–102 (2013).
- Choi, J.-W., MacDonald, E. & Wicker, R. Multi-material microstereolithography. *Int. J. Adv. Manuf. Technol.* **49**, 543–551 (2010).
- Choi, J.-W., Kim, H.-C. & Wicker, R. Multi-material stereolithography. *J. Mater. Process. Technol.* **211**, 318–328 (2011).
- Hardin, J. O., Ober, T. J., Valentine, A. D. & Lewis, J. A. Microfluidic printheads for multimaterial 3D printing of viscoelastic inks. *Adv. Mater.* **27**, 3279–3284 (2015).
- Ober, T. J., Foresti, D. & Lewis, J. A. Active mixing of complex fluids at the microscale. *Proc. Natl Acad. Sci. USA* **112**, 12293–12298 (2015).
- Frutiger, A. *et al.* Capacitive soft strain sensors via multicore-shell fiber printing. *Adv. Mater.* **27**, 2440–2446 (2015).
- Kokkinis, D., Schaffner, M. & Studart, A. R. Multimaterial magnetically assisted 3D printing of composite materials. *Nature Commun.* **6**, 8643 (2015).
- Bartlett, N. W. *et al.* Robot powered by combustion. *Science* **349**, 161–165 (2015).
- This paper highlights the ability to generate graded matrices for soft robots.**
- Zheng, X. *et al.* Design and optimization of a light-emitting diode projection micro-stereolithography three-dimensional manufacturing system. *Rev. Sci. Instrum.* **83**, 125001 (2012).
- Zheng, X. *et al.* Ultralight, ultrastiff mechanical metamaterials. *Science* **344**, 1373–1377 (2014).
- Meza, L. R. *et al.* Resilient 3D hierarchical architected metamaterials. *Proc. Natl Acad. Sci. USA* **112**, 11502–11507 (2015).
- Frenzel, T., Findeisen, C., Kadic, M., Gumbsch, P. & Wegener, M. Tailored buckling microlattices as reusable light-weight shock absorbers. *Adv. Mater.* **28**, 5865–5870 (2016).
- Kinstlinger, I. S. *et al.* Open-source selective laser sintering (OpenSLS) of nylon and biocompatible polycaprolactone. *PLoS ONE* **11**, e0147399 (2016).
- Derby, B. Inkjet printing of functional and structural materials: fluid property requirements, feature stability, and resolution. *Annu. Rev. Mater. Res.* **40**, 395–414 (2010).
- Fromm, J. E. Numerical calculation of the fluid dynamics of drop-on-demand jets. *IBM J. Res. Dev.* **28**, 322–333 (1984).
- Lewis, J. A. Direct ink writing of 3D functional materials. *Adv. Funct. Mater.* **16**, 2193–2204 (2006).
- Zein, I., Hutmacher, D. W., Tan, K. C. & Teoh, S. H. Fused deposition modeling of novel scaffold architectures for tissue engineering applications. *Biomaterials* **23**, 1169–1185 (2002).
- Farahani, R. D., Dubé, M. & Theriault, D. Three-dimensional printing of multifunctional nanocomposites: Manufacturing techniques and applications. *Adv. Mater.* **28**, 5794–5821 (2016).
- Gratson, G. M., Xu, M. & Lewis, J. A. Direct writing of three-dimensional webs. *Nature* **428**, 386 (2004).
- Clausen, A., Wang, F., Jensen, J. S., Sigmund, O. & Lewis, J. A. Topology optimized architectures with programmable Poisson’s ratio over large deformations. *Adv. Mater.* **27**, 5523–5527 (2015).
- Shan, S. *et al.* Multistable architected materials for trapping elastic strain energy. *Adv. Mater.* **27**, 4296–4301 (2015).
- Gladman, A. S., Matsumoto, E. A., Nuzzo, R. G., Mahadevan, L. & Lewis, J. A. Biomimetic 4D printing. *Nature Mater.* **15**, 413–418 (2016).
- Theriault, D., Shepherd, R. F., White, S. R. & Lewis, J. A. Fugitive inks for direct-write assembly of three-dimensional microvascular networks. *Adv. Mater.* **17**, 395–399 (2005).
- Wu, W., Deconinck, A. & Lewis, J. A. Omnidirectional printing of 3D microvascular networks. *Adv. Mater.* **23**, H178–H183 (2011).
- Herschel, W. H. & Bulkley, R. Konsistenzmessungen von Gummi-Benzollösungen. *Kolloid Z.* **39**, 291–300 (1926).
- Farahani, R. D., Lebel, L. L. & Theriault, D. Processing parameters investigation for the fabrication of self-supported and freeform polymeric microstructures using ultraviolet-assisted three-dimensional printing. *J. Micromech. Microeng.* **24**, 055020 (2014).
- Vidimce, K., Wang, S.-P., Ragan-Kelley, J. & Matusik, W. OpenFab: A programmable pipeline for multi-material fabrication. *ACM Trans. Graph.* **32**, 136 (2013).
- Muth, J. T. *et al.* Embedded 3D printing of strain sensors within highly stretchable elastomers. *Adv. Mater.* **26**, 6307–6312 (2014).
- The paper details a method to create soft strain sensors embedded in elastomeric matrices.**
- Bhattacharjee, T. *et al.* Writing in the granular gel medium. *Sci. Adv.* **1**, e1500655 (2015).
- Brackett, D., Ashcroft, I. & Hague, R. Topology optimization for additive manufacturing. In *Solid Freeform Fabrication Symposium* 348–362 (2011).
- Lin, D. *et al.* Three-dimensional printing of complex structures: Man made or

- toward nature? *ACS Nano* **8**, 9710–9715 (2014).
59. Montemayor, L., Chernow, V. & Greer, J. R. Materials by design: Using architecture in material design to reach new property spaces. *MRS Bull.* **40**, 1122–1129 (2015).
 60. Wegst, U. G. K., Bai, H., Saiz, E., Tomsia, A. P. & Ritchie, R. O. Bioinspired structural materials. *Nature Mater.* **14**, 23–36 (2015).
 61. Launey, M. E., Buehler, M. J. & Ritchie, R. O. On the mechanistic origins of toughness in bone. *Annu. Rev. Mater. Res.* **40**, 25–53 (2010).
 62. Gibson, L. J. The hierarchical structure and mechanics of plant materials. *J. R. Soc. Interface* **9**, 2749–2766 (2012).
 63. Martin, J. J., Fiore, B. E. & Erb, R. M. Designing bioinspired composite reinforcement architectures via 3D magnetic printing. *Nature Commun.* **6**, 8641 (2015). doi:10.1038/ncomms9641
 - This paper demonstrates the power of combining 3D printing with external magnetic fields to produce oriented composite architectures.**
 64. Dimas, L. S., Bratzel, G. H., Eylon, I. & Buehler, M. J. Tough composites inspired by mineralized natural materials: Computation, 3D printing, and testing. *Adv. Funct. Mater.* **23**, 4629–4638 (2013).
 65. Matsuzaki, R. *et al.* Three-dimensional printing of continuous-fiber composites by in-nozzle impregnation. *Sci. Rep.* **6**, 23058 (2016).
 66. Schaedler, T. A. *et al.* Ultralight metallic microlattices. *Science* **334**, 962–965 (2011).
 67. Duoss, E. B. *et al.* Three-dimensional printing of elastomeric, cellular architectures with negative stiffness. *Adv. Funct. Mater.* **24**, 4905–4913 (2014).
 68. Hu, J., Meng, H., Li, G. & Ibekwe, S. I. A review of stimuli-responsive polymers for smart textile applications. *Smart Mater. Struct.* **21**, 053001 (2012).
 69. Felton, S., Tolley, M., Demaine, E., Rus, D. & Wood, R. A method for building self-folding machines. *Science* **345**, 644–646 (2014).
 70. Randall, C. L., Gultepe, E. & Gracias, D. H. Self-folding devices and materials for biomedical applications. *Trends Biotechnol.* **30**, 138–146 (2012).
 71. Liu, Y., Boyles, J. K., Genzer, J. & Dickey, M. D. Self-folding of polymer sheets using local light absorption. *Soft Matter* **8**, 1764–1769 (2012).
 72. Tibbits, S. 4D printing: Multi-material shape change. *Architect. Des.* **84**, 116–121 (2014).
 - This paper describes the first embodiment of 4D printing.**
 73. Raviv, D. *et al.* Active printed materials for complex self-evolving deformations. *Sci. Rep.* **4**, 7422 (2014).
 74. Ge, Q., Qi, H. J. & Dunn, M. L. Active materials by four-dimension printing. *Appl. Phys. Lett.* **103**, 131901 (2013).
 75. Ge, Q., Dunn, C. K., Qi, H. J. & Dunn, M. L. Active origami by 4D printing. *Smart Mater. Struct.* **23**, 094007 (2014).
 76. Mao, Y. *et al.* Sequential self-folding structures by 3D printed digital shape memory polymers. *Sci. Rep.* **5**, 13616 (2015).
 77. Mao, Y. *et al.* 3D printed reversible shape changing components with stimuli responsive materials. *Sci. Rep.* **6**, 24761 (2016).
 78. Burgert, I. & Fratzl, P. Actuation systems in plants as prototypes for bioinspired devices. *Phil. Trans. R. Soc. A* **367**, 1541–1557 (2009).
 79. Guo, Q. *et al.* Fast nastic motion of plants and bioinspired structures. *J. R. Soc. Interface* **12**, 20150598 (2015).
 80. Ilievski, F., Mazzeo, A. D., Shepherd, R. F., Chen, X. & Whitesides, G. M. Soft robotics for chemists. *Angew. Chem. Int. Edn Engl.* **50**, 1890–1895 (2011).
 81. Bauer, S. *et al.* 25th anniversary article: A soft future: From robots and sensor skin to energy harvesters. *Adv. Mater.* **26**, 149–162 (2014).
 82. Rus, D. & Tolley, M. T. Design, fabrication and control of soft robots. *Nature* **521**, 467–475 (2015).
 83. Yamada, T. *et al.* A stretchable carbon nanotube strain sensor for human-motion detection. *Nature Nanotechnol.* **6**, 296–301 (2011).
 84. Lu, N., Lu, C., Yang, S. & Rogers, J. Highly sensitive skin-mountable strain gauges based entirely on elastomers. *Adv. Funct. Mater.* **22**, 4044–4050 (2012).
 85. Lee, C., Jug, L. & Meng, E. High strain biocompatible polydimethylsiloxane-based conductive graphene and multiwalled carbon nanotube nanocomposite strain sensors. *Appl. Phys. Lett.* **102**, 183511 (2013).
 86. Majidi, C., Kramer, R. & Wood, R. J. A non-differential elastomer curvature sensor for softer-than-skin electronics. *Smart Mater. Struct.* **20**, 105017 (2011).
 87. Park, Y.-L., Chen, B. & Wood, R. J. Design and fabrication of soft artificial skin using embedded microchannels and liquid conductors. *IEEE Sens. J.* **12**, 2711–2718 (2012).
 88. Chossat, J. B., Park, Y.-L., Wood, R. J. & Duchaine, V. A soft strain sensor based on ionic and metal liquids. *IEEE Sens. J.* **13**, 3405–3414 (2013).
 89. Sekitani, T. *et al.* A rubberlike stretchable active matrix using elastic conductors. *Science* **321**, 1468–1472 (2008).
 90. Matsuhsa, N. *et al.* Printable elastic conductors with a high conductivity for electronic textile applications. *Nature Commun.* **6**, 7461 (2015).
 91. Boley, J. W., White, E. L., Chiu, G. T. C. & Kramer, R. K. Direct writing of gallium-indium alloy for stretchable electronics. *Adv. Funct. Mater.* **24**, 3501–3507 (2014).
 92. Lee, H., Xia, C. & Fang, N. X. First jump of microgel: actuation speed enhancement by elastic instability. *Soft Matter* **6**, 4342–4345 (2010).
 93. Palleau, E., Morales, D., Dickey, M. D. & Velev, O. D. Reversible patterning and actuation of hydrogels by electrically assisted ionoprinting. *Nature Commun.* **4**, 2257 (2013).
 94. Ionov, L. Biomimetic hydrogel-based actuating systems. *Adv. Funct. Mater.* **23**, 4555–4570 (2013).
 95. Brown, E. *et al.* Universal robotic gripper based on the jamming of granular material. *Proc. Natl Acad. Sci. USA* **107**, 18809–18814 (2010).
 96. Anderson, I. A., Gisby, T. A., McKay, T. G., O'Brien, B. M. & Calius, E. P. Multi-functional dielectric elastomer artificial muscles for soft and smart machines. *J. Appl. Phys.* **112**, 041101 (2012).
 97. Suzumori, K. Elastic materials producing compliant robots. *Rob. Auton. Syst.* **18**, 135–140 (1996).
 98. Peele, B. N., Wallin, T. J., Zhao, H. & Shepherd, R. F. 3D printing antagonistic systems of artificial muscle using projection stereolithography. *Bioinspir. Biomim.* **10**, 055003 (2015).
 99. Robinson, S. S. *et al.* Integrated soft sensors and elastomeric actuators for tactile machines with kinesthetic sense. *Extreme Mech. Lett.* **5**, 47–53 (2015).
 100. MacCurdy, R., Katzschmann, R., Kim, Y. & Rus, D. Printable hydraulics: A method for fabricating robots by 3D co-printing solids and liquids. Preprint at <http://arxiv.org/abs/1512.03744> (2015).
 101. Wehner, M. *et al.* An integrated design and fabrication strategy for entirely soft, autonomous robots. *Nature* **536**, 451–455 (2016).

Acknowledgements We thank J. Raney, J. Muth and M. Skylar-Scott for their valuable insights, and the Wyss Institute for Biologically Inspired Engineering.

Author Information Reprints and permissions information is available at www.nature.com/reprints. The authors declare competing financial interests, see go.nature.com/2gopvxx. Readers are welcome to comment on the online version of this paper at go.nature.com/2gopvxx. Correspondence and requests for materials should be addressed to J.A.L. (jalewis@seas.harvard.edu).

Reviewer information *Nature* thanks B. Derby and D. Therriault for their contributions to the peer review of this work.